

# VALIDATION OF FINITE-ELEMENT MODEL OF THOR-NT LOWER ABDOMEN

**Romain Desbats**

**Sabine Compigne**

**Ernesto Mottola**

Toyota Motor Europe NV/SA

Belgium

**Mitsutoshi Masuda**

Toyota Motor Corporation

Japan

Paper Number 13-0339

## ABSTRACT

THOR is expected to be the next regulatory frontal impact crash test dummy. It brings substantial biofidelity improvements and additional measurement capabilities compared to the current Hybrid III dummy. However, THOR-NT lower abdomen biofidelity was reported as limited. To improve it, numerical modelling would allow the evaluation of several design solutions but would need a validated THOR Finite Element (FE) model. Under NHTSA initiative, a THOR FE model was developed and made publically available. The current study aimed at validating the lower abdomen of the THOR-NT version 1.0 FE model issued in 2011. Impactor and seatbelt tests performed on THOR-NT according to published Post Mortem Human Subject test set-ups were simulated using LS-DYNA FE code. Limitations of the current material model used for the abdomen foam block were highlighted and additional material characterisation was performed to take into account foam compression rate sensitivity. Abdomen model response was improved for rigid-bar load type, whereas validation under seat belt tests suggested that additional investigations should be carried out including the validation of the pelvis flesh model.

## INTRODUCTION

THOR abdomen biofidelity specifications were defined from Cavanaugh et al. (1986) Post Mortem Human Subject (PMHS) tests. A Biofidelity corridor was defined from them by Hardy et al. (2001) that THOR response only fulfills until 80 mm of penetration as shown by Hanen et al. (2011). This test configuration aimed at simulating the impact between a car occupant and the lower rim of the steering wheel. However, it did not consider the dummy biofidelity under seat belt loading for restrained drivers and other occupants in the car. In addition, Elhagediab et al. (1998) found that the seat belt was reported as the most common source of AIS3+ injuries to the digestive system.

Hanen et al. (2011) evaluated THOR-NT lower abdomen mechanical response under seat belt load and found that the dummy abdomen did not match the PMHS corridors defined by Foster et al. (2006). Proposals for modifications to the THOR lower abdomen were presented by Masuda and Compigne (2012). The prototype response was more biofidelic but could be further improved by tuning its abdomen block characteristics and looking at the interaction with other body parts (upper abdomen, pelvis flesh). This can be efficiently done using the THOR FE model. As a first requirement to this approach, the current abdomen FE model was validated comparing its lower abdomen response to Hanen et al. (2011) experiments on THOR-NT crash test dummy. The comparison of the original model response with the test results is presented in this paper together with improvements of the abdomen foam material properties. Finally, the modified model was evaluated against the same test data.

## METHODS

Tests performed by Hanen et al. (2011) on THOR-NT were simulated with THOR FE model under LS-DYNA® software.

### Test set-ups

THOR-NT lower abdomen mechanical response was assessed by Hanen et al. (2011) under two kinds of dynamic loading conditions:

- Impactor tests according to Cavanaugh et al. (1986) test set-up were performed with a 25 mm diameter rigid bar of length 300 mm and mass 32 kg. Initial speed was set at 3 and 6.1 m/s. Measured speeds during tests are presented in Table 1. The back of the dummy was unrestrained (Figure 1.a),
- Seatbelt tests according to Foster et al. (2006) test set-up were reproduced with either one or two pretensioners retracting the seatbelt. In that case the back of the dummy was fixed (See Figure 1.b). The retraction velocity profiles for the two conditions are

shown on Figure 1 and peak velocity values are reported in Table 2.



Figure 1. (a) Impactor test from Hanen et al. (2011), (b) Seatbelt test from Hanen et al. (2011).

Table 1.  
Rigid-bar tests

Theoretical speed (m/s)	Impactor mass	Measured velocity (m/s)
Low speed (3 m/s)	TME-1	3.03
	TME-3	2.75
High speed (6.1 m/s)	TME-4	6.16
	TME-5	6.15

Table 2.  
Peak retraction velocities for seatbelt tests

Pretensioner	Test Id	Peak velocity (m/s)
A (high speed)	TAP-02	11.4
	TAP-03	10.8
B (low speed)	TAP-04	4.9
	TAP-05	5.1

**In rigid-bar simulation set-up**, a mass of 32kg was assigned to a cylindrical rigid bar modeled with solid elements having steel material properties, subjected to a 3 m/s or 6.1 m/s initial velocity (average speed of each impactor test configuration was considered). The dummy was positioned on a plane surface with outstretched legs. His lumbar spine joint was in slouched position (9° between lumbar bracket and pelvis bracket). The gravity was applied alone during 500 ms before the impact in order to reproduce the interaction between the dummy pelvis flesh and the ground using an AUTOMATIC\_SURFACE\_TO\_SURFACE contact. An AUTOMATIC\_SURFACE\_TO\_SURFACE contact was also defined between the impactor and dummy components - jacket, front foam block and pelvis flesh. A 0.185 friction coefficient was defined in this contact.

Impact forces were extracted from the contact between the rigid-bar and the dummy. The deflection was calculated by subtracting the longitudinal displacement of THOR abdomen rigid back plate

node to the one of an impactor node. Low speed impact simulation was compared to TME-1 and TME-3 tests. High speed impact simulation was compared to TME-4 and TME-5 tests.

**In seat belt simulation set-up**, the dummy was positioned on a plane surface, its back tangent to a vertical plane surface. No gravity was applied since the dummy / ground interaction was believed to be less important than in the impactor tests due to the limited dummy displacement. The seatbelt is modelled with shell elements with membrane formulation. The material model is FABRIC defined as locally orthotropic with Young's modulus of 4.201GPa in longitudinal and normal directions (0 in transverse direction) and Poisson's ratio of 0.4 in all the directions.

An AUTOMATIC\_SURFACE\_TO\_SURFACE contact was defined between the seatbelt shell elements and a set of dummy parts including the pelvis, the lower jacket and the front foam block of the dummy. This contact included a 0.2875 friction coefficient. The seatbelt velocity profiles specific to each test (Figure 2) was applied as imposed motion to a rigid bar pulling the seatbelt backwards.

The seatbelt force was computed by adding the output forces of two CROSS\_SECTIONS. They consisted of shell elements taken on both sides of the seat belt at similar levels than the two seat belt load cells used in tests. The penetration was calculated by subtracting the longitudinal displacement of a node placed on the pelvis flesh side to the one of a seat belt node positioned at the dummy umbilicus.

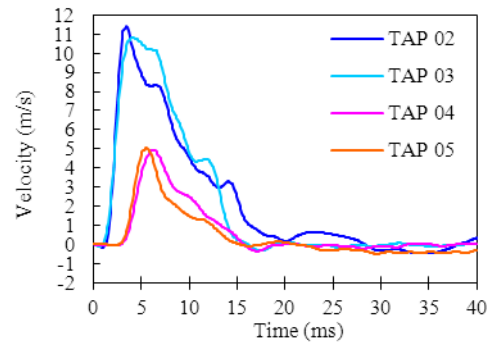


Figure 2. Seatbelt retraction speeds for pretensioner "A" (TAP-02 & TAP-03) and pretensioner "B" (TAP-04 & TAP-05).

Figure 3 and Figure 4 show simulation set-ups for impactor and seatbelt loading respectively. Models were run using the LS-DYNA explicit Finite Element code Version 971sR4 under 8 CPUs with SMP processing.

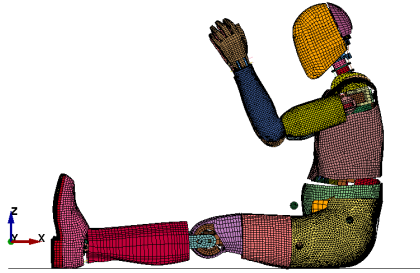


Figure 3. Simulation set-up for rigid-bar tests.

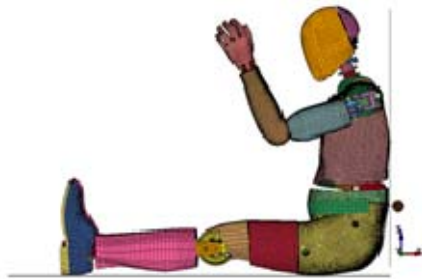


Figure 4. Simulation set-up for seatbelt tests.

### Lower abdomen front foam block modelling

The dummy lower abdomen is made of two types of foam. The outer layer is a very soft open cell foam known as charcoal polyester while the inner layer is a stiffer sponge rubber (GESAC, 1998; Figure 5).

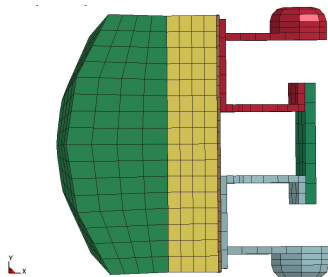


Figure 5. THOR-NT lower abdomen (Top view: outer layer in green, inner layer in yellow).

The material model MAT\_LOW\_DENSITY\_FOAM (057) was used in the THOR model of the front foam block (outer layer). A viscoelastic formulation is included in this material card to account for strain rate effect. However, the material card does not allow the user to define actual stress factor versus strain rate but only some viscoelastic parameters which are difficult to tune. The stress-strain curve implemented in the model corresponded to a strain rate of  $35 \text{ s}^{-1}$ . This curve was obtained from a compression test at  $1.8 \text{ m/s}$  on a  $50.8 \text{ mm}$  side cube. The unloading phase is also computed from this curve.

However, strain rate peaks between  $50 \text{ s}^{-1}$  and  $200 \text{ s}^{-1}$  were observed in rigid-bar loading and between  $70 \text{ s}^{-1}$  and  $420 \text{ s}^{-1}$  in seat belt loading. Therefore, it was thought useful to use MAT\_FU\_CHANG\_FOAM (083) model (Serifi et al., 2003; Croop et al., 2009) instead of MAT\_057 to model the foam strain rate effect. It can also be noticed that the upper abdomen front foam block which is made of same foam as the lower abdomen front block used already MAT\_083 formulation for quasi-static loading,  $24$  and  $36 \text{ s}^{-1}$  strain rates. For the lower abdomen front foam block, nine stress-strain curves were input in this model based on dynamic compression test data performed on THOR dummy abdomen foam samples (see APPENDIX 3).

Five curves ( $83 \text{ s}^{-1}$  to  $304 \text{ s}^{-1}$ ) were defined from the experiments and four ( $10 \text{ s}^{-1}$  to  $60 \text{ s}^{-1}$ ) were computed from the experimental ones using Croop et al. (2009) linear relationship between Yield stress and strain rate logarithm.

Figure 6 shows the curves entered in the new model compared to the one in the initial model.

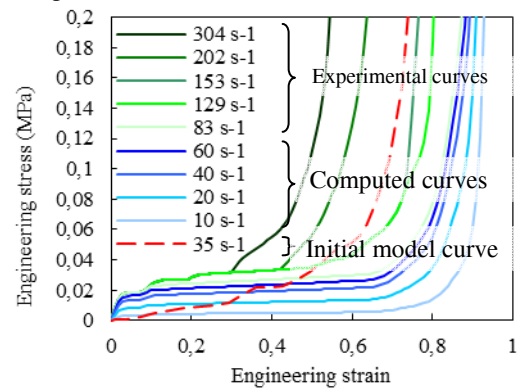


Figure 6. Stress-strain curves implemented in MAT\_083 for front abdominal foam block.

### Other model improvements

The jacket strap passing in between the dummy legs was added to the model as shown in Figure 7. It was connected to the rest of the jacket by merging their nodes at the extremities of the strap. Material properties of the jacket were applied to the strap.

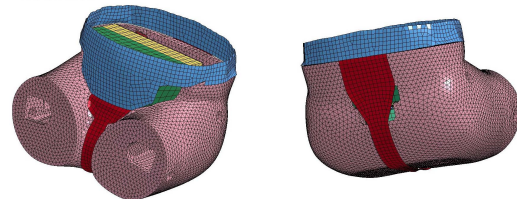


Figure 7. Jacket strap model (in red).

Due to unrealistic penetration between the abdomen back plate and the front foam block, the front foam was covered by NULL shell elements to prevent this phenomenon as shown in Figure 8.

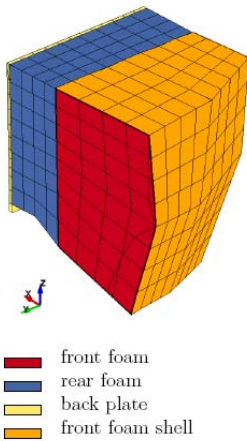


Figure 8. Section view of the lower abdomen with front foam block coated with NULL elements.

## RESULTS

In total, 6 simulations were conducted on the initial and the modified THOR models: 2 conditions for rigid bar tests and 4 conditions for seat belt tests. APPENDIX 1 and APPENDIX 2 show pictures of simulation animations and corresponding test videos.

### Rigid-bar impact simulations

**With the initial model**, the rigid-bar simulation results showed a too high abdominal force peak of the lower abdomen when comparing the tests and the simulations (Figure 9 and Figure 10). At low speed impact, the simulated peak force was from 30% to 38% higher than TME-1 and TME-3 results respectively. High speed impact simulations showed a 51% to 80% higher peak force than tests TME-4 and TME-5 respectively. It was found that it was the consequence of the contact between the pelvis flesh and the rigid-bar. Contact between the impactor and the pelvis flesh was observed at 33 ms in the 3 m/s tests and simulation. In the simulation this contact led to a sharpest force peak of 1000 N higher than in the tests. At 6.1 m/s impact, the contact was observed at 14 ms for both the tests and the simulation. In the simulation, the contact force with the pelvis flesh contributes by 70% to the force peak.

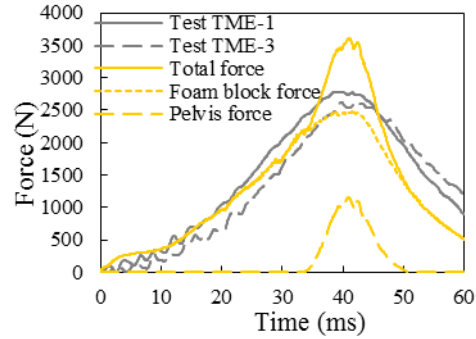


Figure 9. Force-time response curves of the initial model versus the tests for 3 m/s rigid-bar impacts (Total force= Foam block force + Pelvis force).

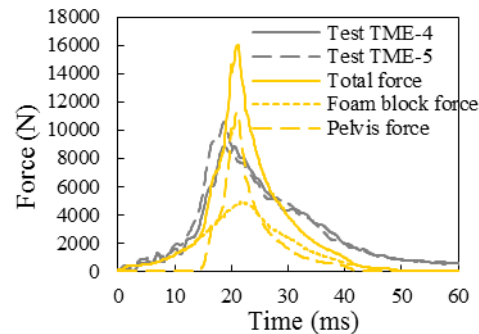
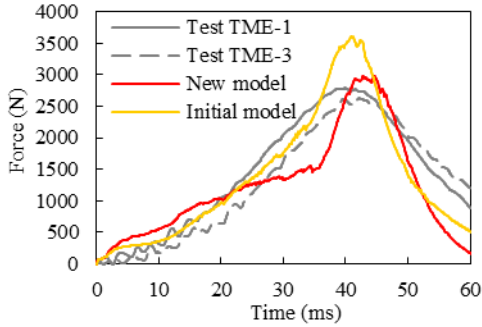


Figure 10. Force-time response curves of the initial model versus the tests for 6.1 m/s rigid-bar impacts (Total force= Foam block force + Pelvis force).

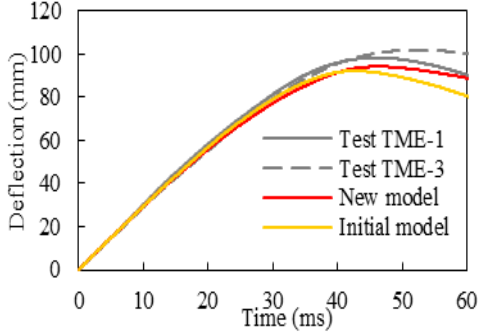
**With the implementation of new material model**, the impact peak force for the 3 m/s impact was decreased and the deflection peak slightly increased (Table 3). A higher force was obtained during the first 20 ms (Figure 11a). In addition, a change in force-time slope was observed at the time the rigid bar impacted the pelvis flesh which was not observed in tests. This effect could also be seen on the force-deflection curve (Figure 11c). The deflection curve matched well the test data and its peak was just slightly above the initial model one (Figure 11b).

**Table 3.**  
Low speed impactor test and simulation peaks

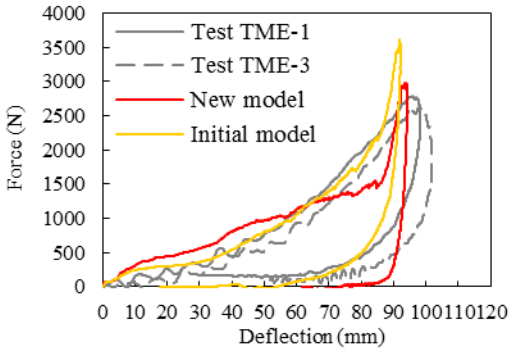
Test/Simulation Id	Force peak (N)	Deflection peak (mm)
TME-1	2758	98
TME-3	2625	102
Initial model	3614	92
New model	2984	94



(a) Force-time responses



(b) Deflection-time responses



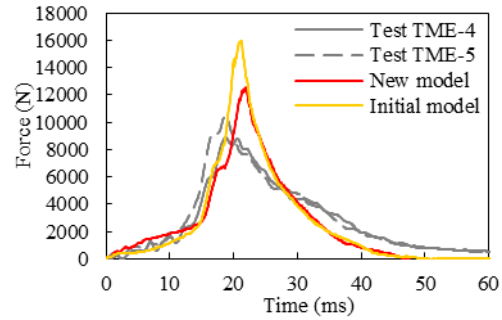
(c) Force-deflection responses

Figure 11. 3 m/s rigid-bar simulation versus test results.

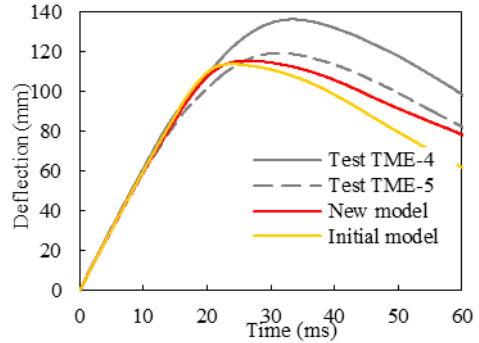
At 6.1 m/s, the new model decreased the peak force by 21%, more in line with test results (Table 4, Figure 12a). Regarding deflection peak values and profiles, the new simulation was closer to the test data (Table 4, Figure 12b). The force-deflection responses are overlaid in Figure 12c. In the simulations, the maximum deflection was obtained at almost the maximum force whereas in the tests, the deflection peaks occurred 10 ms later.

**Table 4.**  
High speed impactor test and simulation peaks

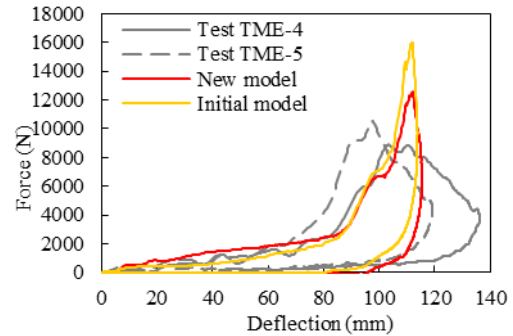
Test/Simulation Id.	Force peak (N)	Deflection peak (mm)
TME-4	8875	136
TME-5	10565	119
Initial model	15985	114
New model	12582	115



(a) Force-time responses



(b) Deflection-time responses



(c) Force-deflection responses

Figure 12. 6.1 m/s rigid-bar simulation versus test results.

### Seatbelt simulations

**Low speed results** for the initial and the new model results are overlaid with test results in Figure 13. The peak values are compared in Table 5. The initial model force result was closer to test data

even though the force magnitude was too high. The beginning of the loading phase showed that the old and new simulation profiles were similar (Figure 13a). The deflection profiles were similar in shape between the old and new simulations, but overall the new simulation showed less deflection, in contradiction with test data (Figure 13b). The force-deflection response had a worse correlation with test data (Figure 13c).

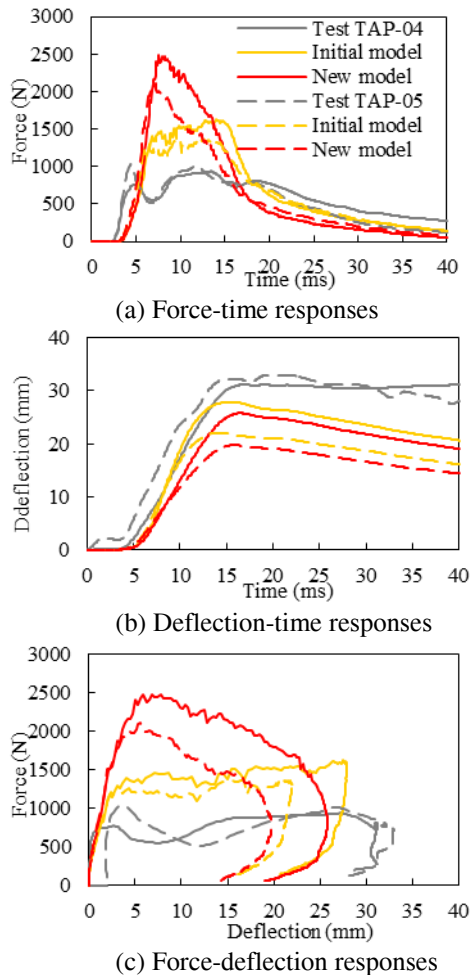


Figure 13. Low speed seat belt simulation versus test results.

**Table 5.**  
Low speed seatbelt test and simulation peaks

Test/Simulation Id.	Force peak (N)	Deflection peak (mm)
TAP-04	938	31
Initial model	1623	28
New model	2483	26
TAP-05	1038	33
Initial model	1365	22
New model	2104	20

**High speed simulations** are overlaid with test results in Figure 14 and peak values are compared in Table 6. At the beginning of the loading phase the force profile of old and new simulations matched test data. The force peak was higher for the new simulation and appeared earlier. In the unloading phase, the new simulation matched better TAP-02 curve whereas the old simulation results were closer to TAP-03 ones (Figure 14a). Regarding the deflection profile (Figure 14b), the new simulation showed higher deflection values in line with test data. Comparing the force-deflection curve (Figure 14c), the old simulation curve shape correlated better with the test data due to a force response closer to the tests.

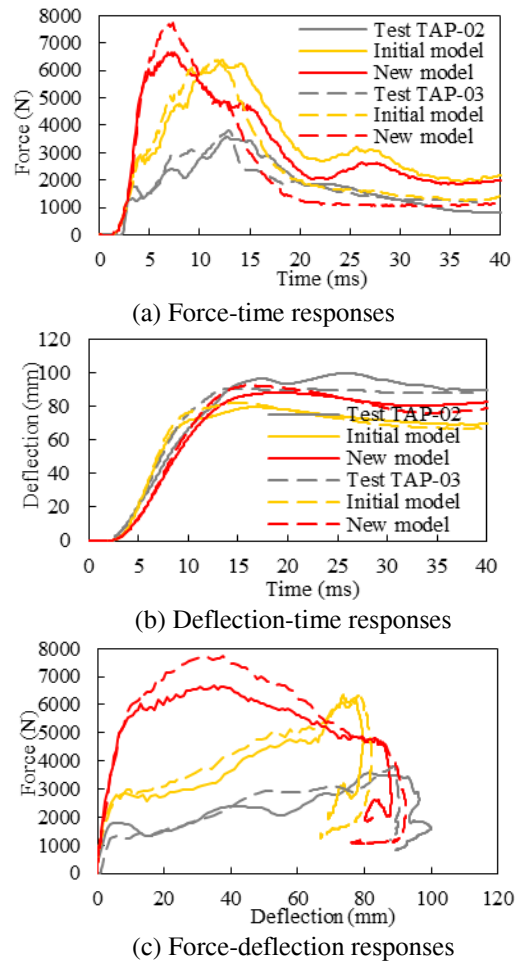


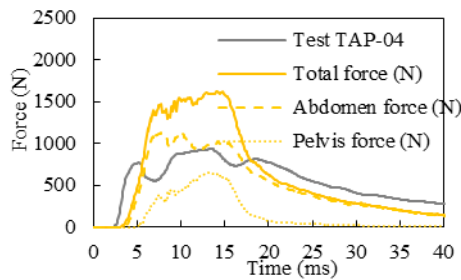
Figure 14. High speed seat belt simulation versus test results.

**Table 6.**  
**High speed seatbelt test and simulation peaks**

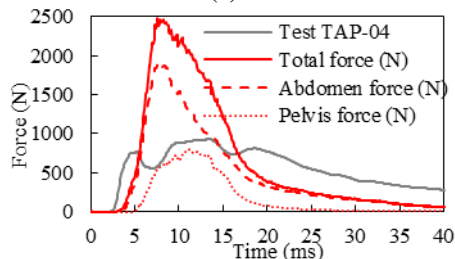
Test/Simulation Id.	Force peak (N)	Deflection peak (mm)
TAP-02	3573	100
Initial model	6381	80
New model	6663	88
TAP-03	3811	91
Initial model	6405	82
New model	7748	92

**The comparison of the force distribution**

between the abdomen and the pelvis shows that for lowest retraction speed (5 m/s), the force due to the abdomen was higher than the one due to the pelvis in both models (Figure 15). This was not the case for higher retraction speed (10 m/s) for which the pelvis force was twice as high as the abdomen force in the initial model and of similar magnitude than the abdomen force in the new model (Figure 16).

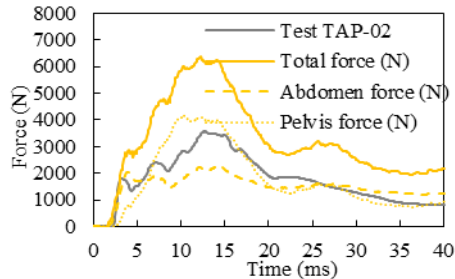


(a) Initial model

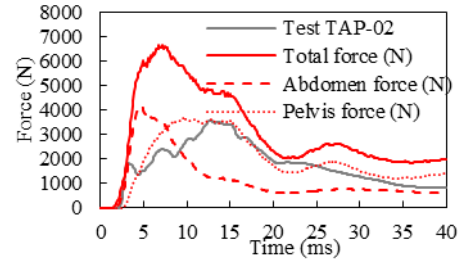


(b) New model

Figure 15. Force distribution between abdomen and pelvis for low speed seat belt simulations.



(a) Initial model



(b) New model

Figure 16. Force distribution between abdomen and pelvis for high speed seat belt simulations, (Total force= Foam block force + Pelvis force).

**DISCUSSION**

**Foam material characterization**

The material characterization of the front foam block of the dummy had some limitations in terms of the range of strain rates tested. Strain rates below  $83 \text{ s}^{-1}$  could not be tested due to the test equipment used and the size of the foam samples. Therefore the abdomen behaviour for low strain rates could only be calculated from the higher strain rate curves. This was based on defining new yield stress values for missing strain rate under the observation that foam yield stress varied linearly with the logarithm of the strain rate (Croop et al., 2009). The lowest strain rate curve ( $83 \text{ s}^{-1}$ ) obtained in test was multiplied by a factor chosen to make the new curve passing through the calculated yield stress value for the considered strain rate. The fact that experimental GESAC's curve at  $35 \text{ s}^{-1}$  did not lie in between the  $20$  and  $40 \text{ s}^{-1}$  curves was not explained but may show an issue with the method used to calculate the stress-strain curves at lower strain rates. However, this might have also been caused by test data obtained from small sample sizes tested at quite high strain rates ( $83 \text{ s}^{-1}$  and above).

**THOR abdomen model validation**

In future, it appears necessary to carry out additional impact tests on the dummy abdomen without any interference with the pelvis flesh. Interferences with pelvis were seen in all the tests performed so far which did not allow to identify the contribution of the abdomen and the pelvis in the total force and deflection.

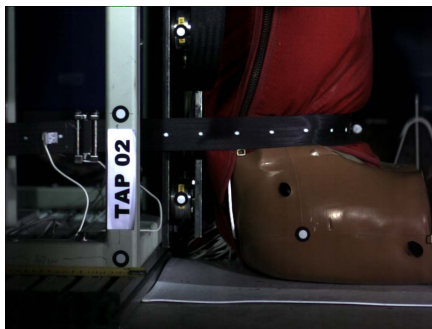
**Impactor test validation limitations**

From actual test videos it seems that the impactor was higher than its theoretical position. This caused the impactor to slip above the pelvis flesh. This

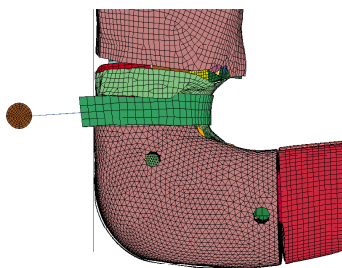
phenomenon happened in one of the two high speed rigid-bar tests (TME-04) but not in the simulation for which a higher peak force was recorded due to the contact with the pelvis flesh.

### Seat belt test validation limitations

The simulation validation was not improved by the new abdomen foam properties despite the high strain rates encountered by the abdomen elements (between  $50 \text{ s}^{-1}$  to  $200 \text{ s}^{-1}$  for the rigid-bar impacts and  $70 \text{ s}^{-1}$  to  $420 \text{ s}^{-1}$  for the seat belt loading) which initially led us to hypothesize that additional strain rate curves should have improved the abdomen response. However, it seems that the interaction between the seat belt and the pelvis flesh played a more predominant role in the dummy lower torso response. The comparison between the test videos and the simulations showed that the deformed shape of the pelvis was not well mimicked by the model. Figure 17 shows that the pelvis side was quite deformed by the seatbelt during the test whereas no major deformation was suggested by the simulation. Additional validation of pelvis material might be recommended in future.



(a) Test at 22 ms



(b) Simulation at 22 ms

Figure 17. Pelvis flesh deformation under high speed seat belt retraction.

### CONCLUSION

The last released version of THOR FE model at the time this work was performed was improved by enhancing the front foam block material definition considering various strain rates. Although the response was improved for rigid bar impactor tests, the new model degraded the correlation with test data for seatbelt loading tests. This showed that the seatbelt test condition was harder to replicate in numerical simulation than the impactor test due to the higher number of influential factors such as dummy back / plate contact, pelvis / seatbelt interaction, seatbelt positioning. A well validated THOR abdomen model requires the validation of the other impacted parts, especially pelvis parts, in the targeted impact conditions.

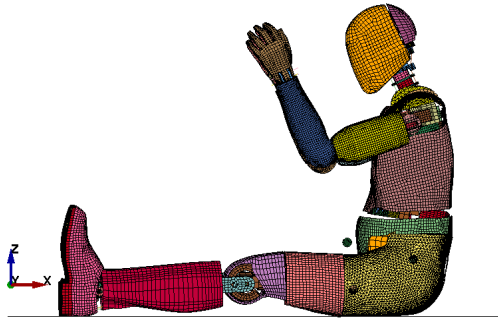
### REFERENCES

- Cavanaugh J., Nyquist G., Goldberg S., and King A. (1986). Lower abdominal tolerance and response. Stapp Car Crash Conference Proceedings, 30:41–63 .
- Croop B. and Lobo H. (2009). Selecting Material Models for the Simulation of Foams in LS-DYNA. In 7th European LS-DYNA Users Conference, 2009.
- Elhagediab A. M., Rouhana S. W. (1998). Patterns of abdominal injury frontal automotive crashes, Paper #98-S1-W-26, Proc. of 16<sup>th</sup> ESV Conference, Windsor, Ontario, Canada, May 31-June4, 1998.
- Foster D., Hardy W., Yang K., King A., and Hashimoto S. (2006). High-speed seatbelt pretensioner loading of the abdomen. Stapp Car Crash Journal, 50:27–51, 2006.
- GESAC, Inc. Test support for finite element modeling of THOR crash test dummy, Contract/Order No: DTRS57-98-P-80521.
- Hanen G. et al. (2011). Contribution to the improvement of crash test dummies in order to decrease abdominal injuries in road accidents, Paper #11-0218, Proc. of 22<sup>nd</sup> ESV Conference, Washington D.C., June 13-16, 2011.
- Hardy W. N., Schneider L. W., Rouhana S. W. (2001). Abdominal impact response to rigid-bar, seat belt and airbag loading. Stapp Car crash Journal, Vol. 45, p.1.

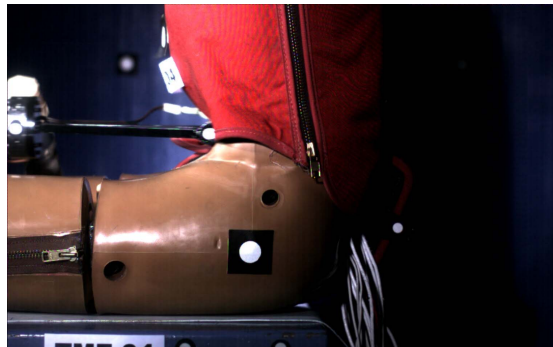
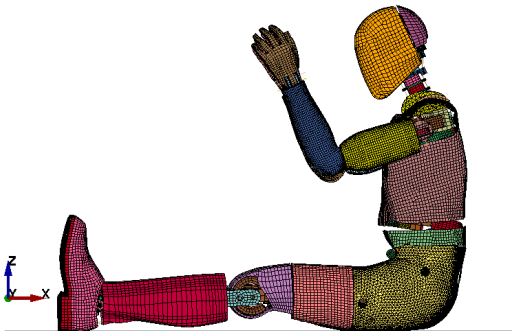
Masuda M., Compigne S. (2012), Dynamic Response of the THOR-NT: Thorax and Abdomen, 2012 SAE-GIM, Washington D.C.

Serifi H., Hirth A., Matthaei S. and Müllershön H.(2003). Modelling of Foams using MAT83 – Preparation and Evaluation of Experimental Data. In 4<sup>th</sup> European LS-DYNA Users Conference, 2003.

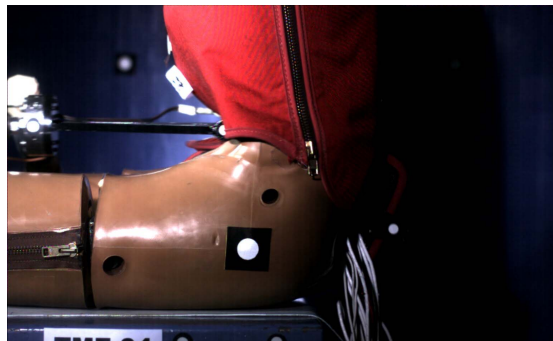
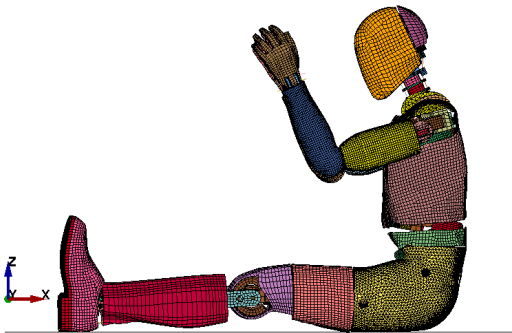
**APPENDIX 1: RIGID-BAR IMPACT SIMULATION VERSUS TEST**



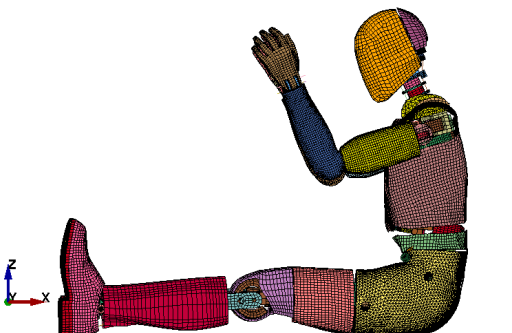
Just before impact



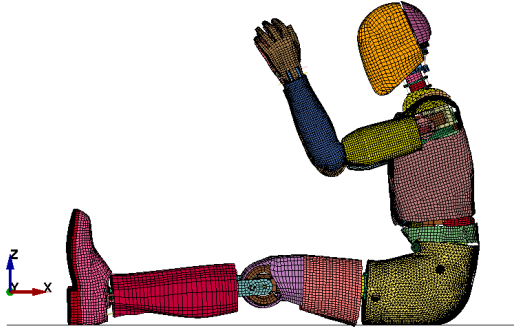
14 ms after impact



18 ms after impact



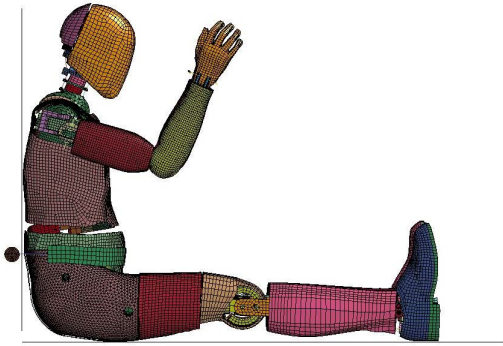
22 ms after impact



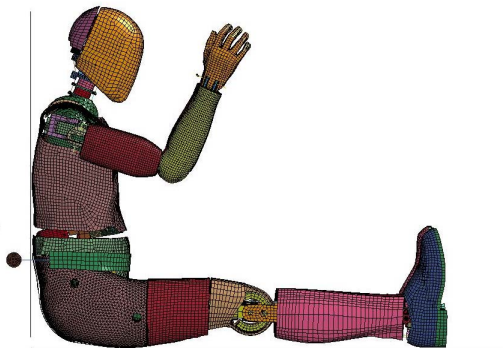
32 ms after impact

Figure 18. 6.1 m/s rigid-bar impact simulation and test (TME-04).

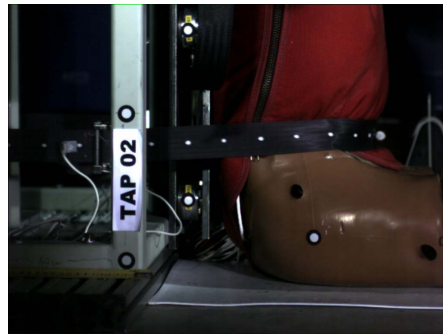
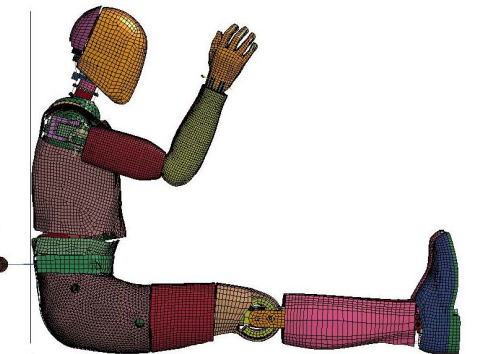
APPENDIX 2: SEAT BELT SIMULATION VERSUS TEST



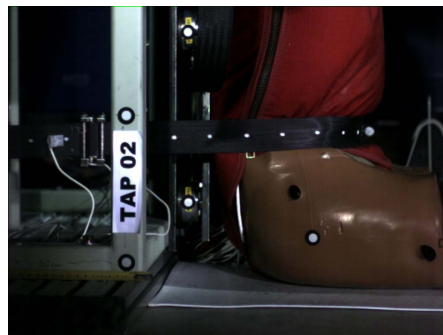
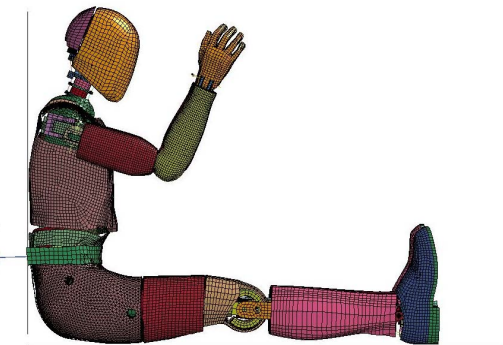
Before seatbelt retraction



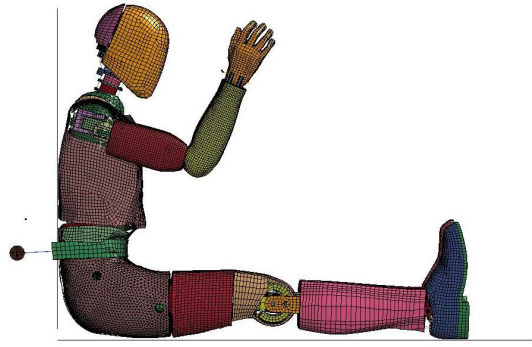
At 4 ms



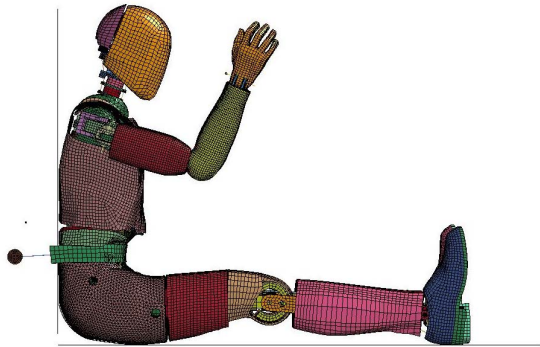
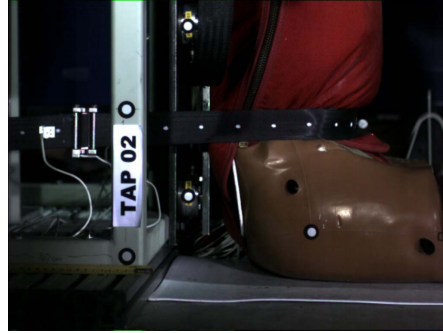
At 8 ms



At 12 ms



At 16 ms



At 20 ms

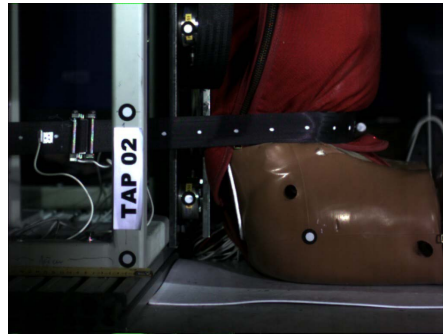


Figure 19. High speed seat belt simulation and test (TAP-02).

### APPENDIX 3: FOAM TESTING SET-UP

#### Samples

Five cylindrical samples from THOR-NT lower abdomen front foam block were tested. Their geometry is described in Table 7.

**Table 7.**  
**Dimensions of tested samples**

samples	Diameter (mm)	Height (mm)
A	36.89	13.07
G1	37.52	23.68
G2	37.76	18.59
G5	45.90	19.87
D5	45.96	16.24

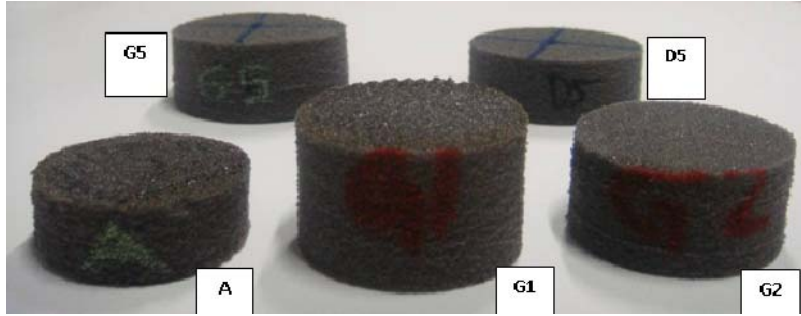


Figure 20. Photo of samples.

#### Test device

A cylinder impactor was used to perform compression tests on the samples according to the test matrix provided in Table 8.

**Table 8.**  
**Test matrix for compression tests on foam samples**

Test Id.	Sample Id.	Impact velocity (m/s)	Impactor mass (kg)	Comments
Test 10	A	2	6	first test on sample A
Test 15	A	2	6	second test on sample A
Test 20	G1	2	6	first test on sample G1
Test 25	G1	2	6	second test on sample G1
Test 30	G2	2.5	6	first test on sample G2
Test 35	G2	2.5	6	second test on sample G2
Test 40	G5	4	6	first test on sample G5
Test 45	G5	4	6	second test on sample G5
Test 50	D5	5	6	first test on sample D5
Test 55	D5	5	6	second test on sample D5